*Original Article*

# Microstrip-Fed 3.04 -10.77 GHz UWB Patch Antenna Design Using CMA and Parametric Study

Pranav Bhatt[1], Komal R. Borisagar[2], Bhavin Sedani[3], Nirali Kotak[4]

[1]*Cyber Security and Digital Forensics, National Forensic Sciences University, Gujarat, India.*
[2]*Graduate School of Engineering and Technology, Gujarat Technological University, Gujarat, India.*
[3]*Electronics and Communication Department- L. D. College of Engineering, Gujarat Technological University, Gujarat, India.*
[4]*Electronics and Communication Department- L. D. College of Engineering, Gujarat Technological University, Gujarat, India.*

[1]pranavm153@gmail.com

*Abstract - This paper proposes the design of an Ultra-wideband antenna covering the entire UWB spectrum. The antenna geometry contains a rectangular stepped patch, FR-4 substrate, and uniquely truncated partial ground plane. All the designs, simulations, and optimizations for the proposed work are done with the help of ANSYS Electronics Desktop 2020 R2. The design process uses characteristic mode analysis (CMA) and parametric analysis. The performance of the proposed antenna is reported with the help of the reflection coefficient curve, voltage standing wave ratio, and smith chart. The designed antenna offers an impedance bandwidth of 7.73GHz (3.04-10.77GHz) for return loss <-10dB.*

*Keywords - Characteristic mode analysis, Partial ground plane, Patch antenna, Step-in change width, UWB.*

## 1. Introduction

The modern Ultra-Wideband communication technology was first introduced in the late 1960s.[1] Nowadays, UWB technology is becoming more attractive for wireless communication applications requiring short-distance, high throughput & high location precision.[2-3] Predicting the need for future communications, the American Federal Communications Commission declared an operating band for UWB signals ranging from 3.1 to 10.6 GHz in 2002.[4] Some of the future applications of UWB will be high-data rate point-to-point communication, smart homes having device initiation with the help of indoor location accuracy, smart commute and transportation, smart shopping, secure wireless payments, and other IoT applications.[5]

Despite having so many advantages, antenna designing for UWB is a highly tedious task compared to designing a narrowband antenna. Like other antennas, the UWB antenna must also provide good VSWR, bandwidth, coverage, and gain over the operating frequency band.[6] In [7], researchers have designed a tunable oval-shaped monopole antenna, covering the entire UWB range with a minor undesirable stop band around 8 GHz; it also covers two other narrow bands, 2.4 GHz and 5.8 GHz, when tuned using the PIN diodes. In [8],

the authors have designed a miniaturized antenna for indoor positioning, covering 919 MHz to 931 MHz in the UHF range and 3.28 GHz to 6.95 GHz in the UWB range. In [9], with the help of characteristics mode theory, researchers have created an 11 x 11 antenna element MIMO array with 484 ports to cover a part of the UWB range (6-8.5 GHz). In [10], authors have designed an optically transparent multiple-input-multiple-output (MIMO) UWB antenna for automotive communication, with an operating range from 2.4 GHz to 11 GHz, isolation of more than 20 dB, and a peak gain of 2 dBi.

This paper illustrates the design of a rectangular patch monopole antenna having microstrip line feeding. The Characteristic Mode Analysis (CMA) and parametric analysis are used here for methodical antenna design and design optimization. The step-in change width method at the microstrip feed input is utilized to create multiple nearby resonances due to the excitation of multiple modes, which produces a wideband. In addition, the partial ground plane technique is also used to increase the bandwidth because the partial ground plane allows back radiation, decreasing the Q factor, i.e., increasing bandwidth. Furthermore, a novel technique of right-angled triangle-shaped truncation of the ground plane is introduced here for bandwidth improvement.

## 2. Basics of CMA
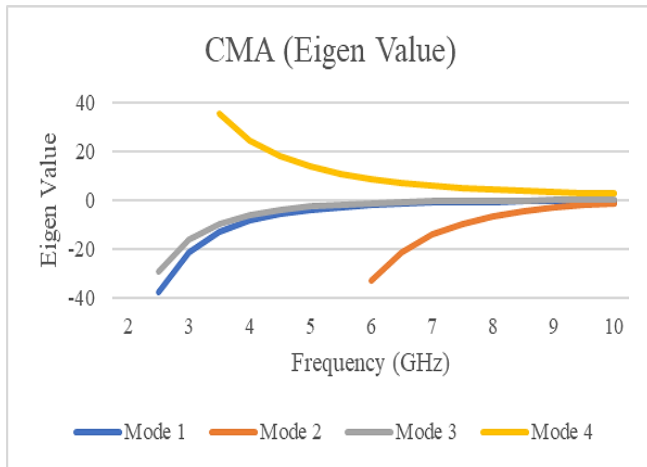


**Fig. 1 Eigenvalue vs. frequency plot for CMA of initial patch geometry**
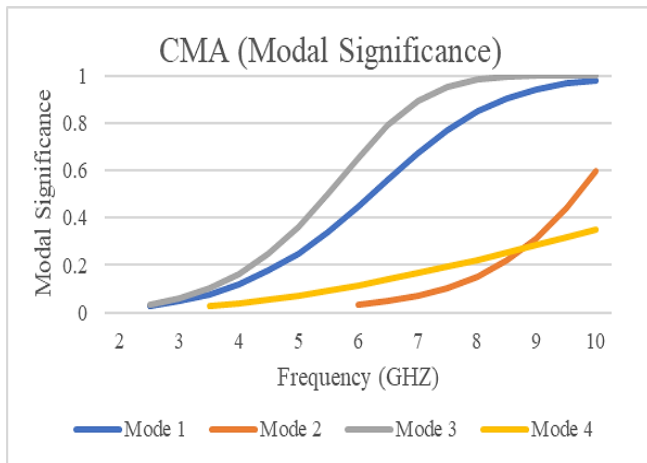


**Fig. 2 Modal significance vs. frequency plot for CMA of initial patch geometry**
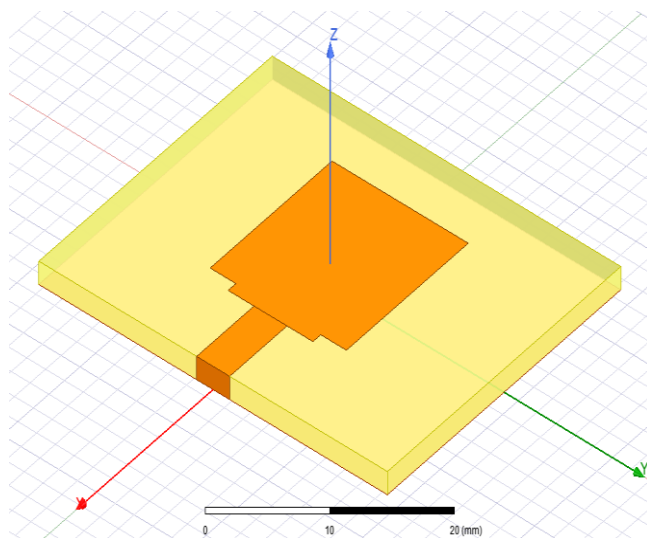


**Fig. 3 3D antenna geometry after the introduction of the first step**

The first mention of the Characteristic Modes (CM) theory in the literature can be found in this research work.[11] But in recent years, it has been in the spotlight in antenna engineering.[12] Any random-shaped conducting body has its natural modes of resonance; CMA uses those modes to indicate the current subsisting patterns in the body.[13] The CMA does not require source excitation of the conducting body to determine the natural modes of resonance, making the designing process easier for designers, especially to find the excitation location for a particular mode and to understand the electromagnetic behaviour of the structure in general. So, in essence, the
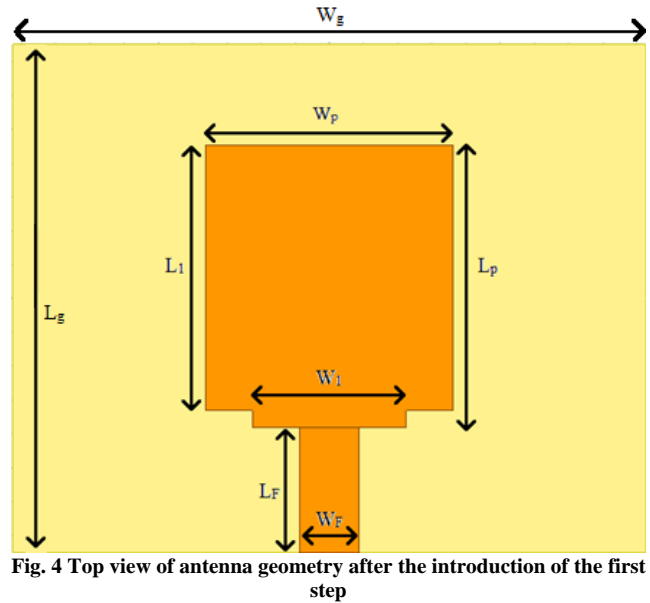


**Fig. 4 Top view of antenna geometry after the introduction of the first step**

**Table 1. Design parameters for the antenna are shown in Figure 4**

| Parameter | Value |
|---|---|
| Width of the patch ($W_p$) | 14.46mm |
| Length of the patch ($L_p$) | 16.66mm |
| Width of patch excluding first steps ($W_1$) | 9mm |
| Length of patch excluding first step ($L_1$) | 15.66mm |
| Substrate height (h) | 1.6mm |
| The relative dielectric constant of the substrate ($\varepsilon_R$) | 4.4 |
| Width of feed line ($W_F$) | 3.5mm |
| Length of feed line ($L_F$) | 7.375mm |
| Width of the ground plane ($W_g$) | 37mm |
| Length of the ground plane ($L_g$) | 30mm |
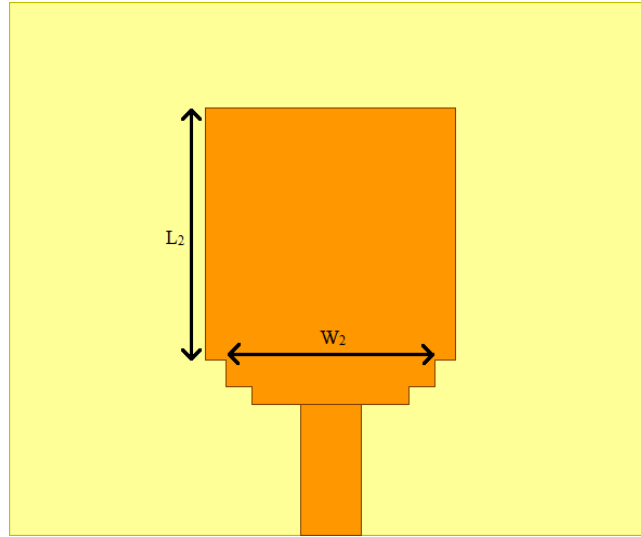
**Fig. 5 Top view of antenna geometry after the introduction of both steps**

CMA provides antenna designers with a systematic and efficient design approach compared to the traditional iterative and inefficient approach.[14] For more information
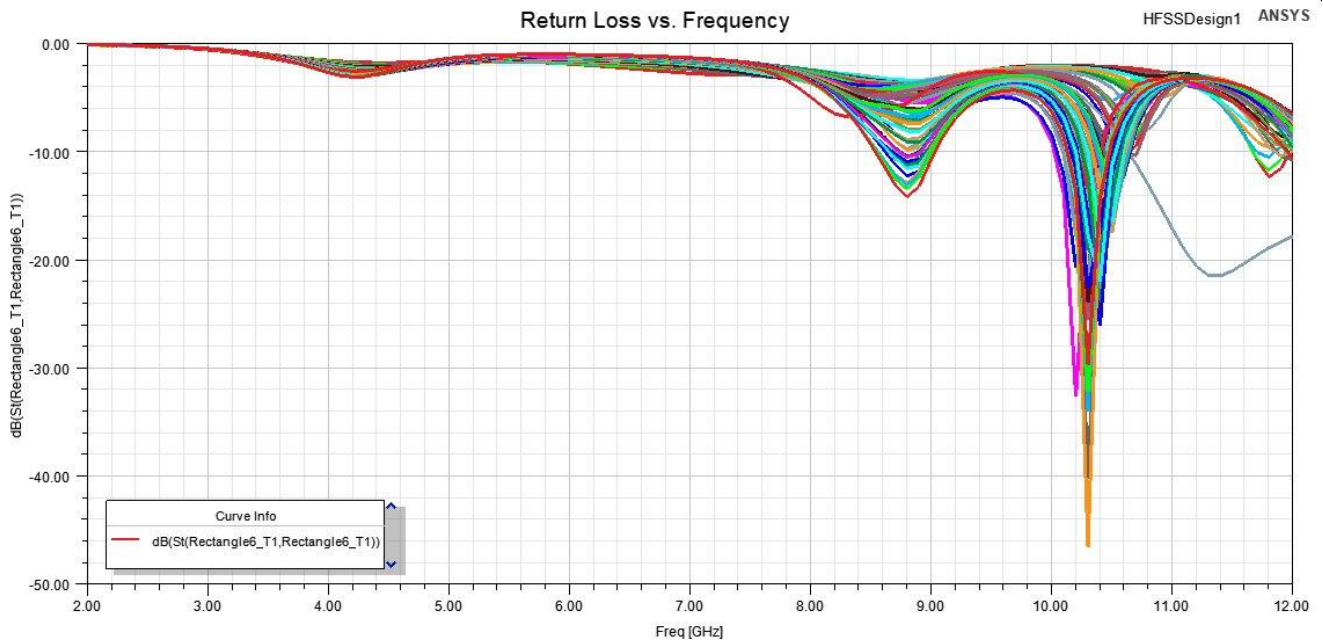


**Fig. 6 Parametric study to find optimum dimensions for the second step**

**Table 2. Dimensions for geometry are shown in Figure 5**

| Parameter | Value |
|---|---|
| Width of patch excluding second steps ($W_2$) | 12mm |
| Length of patch excluding both steps ($L_2$) | 14.16mm |
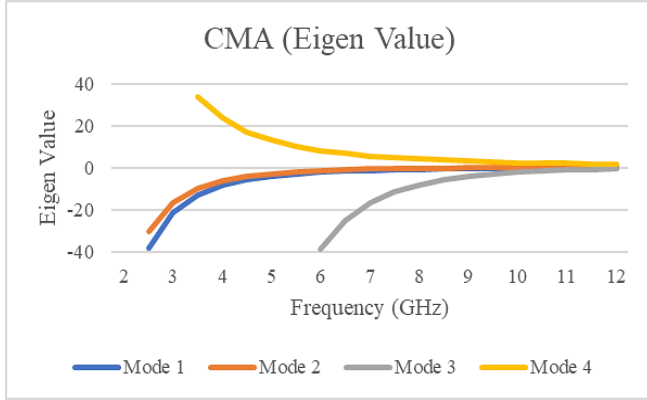
**Fig. 7 Eigenvalue vs. frequency plot for CMA of patch geometry shown in Figure 5**
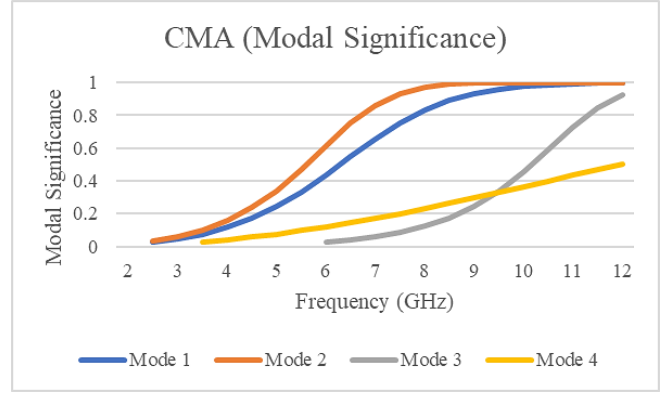


**Fig. 8 Modal significance vs. frequency plot for CMA of patch geometry shown in Figure 5**

refer to these research works.[15-20] The weighted eigenvalue equation for CMA is given:[21]

$$X(\overrightarrow{J_n}) = \lambda_n R(\overrightarrow{J_n}) \tag{1}$$

where $\lambda_n$ is the eigenvalue of $n^{th}$ mode, $\overrightarrow{J_n}$ is eigencurrent of respective $n^{th}$ mode. For the impedance, the equation is:

$$Z = R + jX \tag{2}$$

The weighted sum of the orthogonal components gives the total current on the body:[10-16]

$$\vec{J} = \sum_n \alpha_n \overrightarrow{J_n} = \sum_n \frac{V_n^i \overrightarrow{J_n}}{1+j\lambda_n} \tag{3}$$

where $\alpha_n$ is weighting coefficient of $n^{th}$ mode $V_n^i$ is the excitation coefficient of $n^{th}$ mode. The expression for excitation coefficient is given here:[22]

$$V_n^i = \oiint_s \overrightarrow{J_n} \cdot \overrightarrow{E^i} \, ds \tag{4}$$

where $\overrightarrow{E^i}$ is the input excitation source. The equation for the weighting coefficient is expressed here:[22]

$$\alpha_n = \frac{V_n^i}{1+j\lambda_n} \tag{5}$$

Some parameters are used for the CMA:[22]

$$MS_n = \left| \frac{1}{1+j\lambda_n} \right| \tag{6}$$

where $MS_n$ is the modal significance of $n^{th}$ mode.
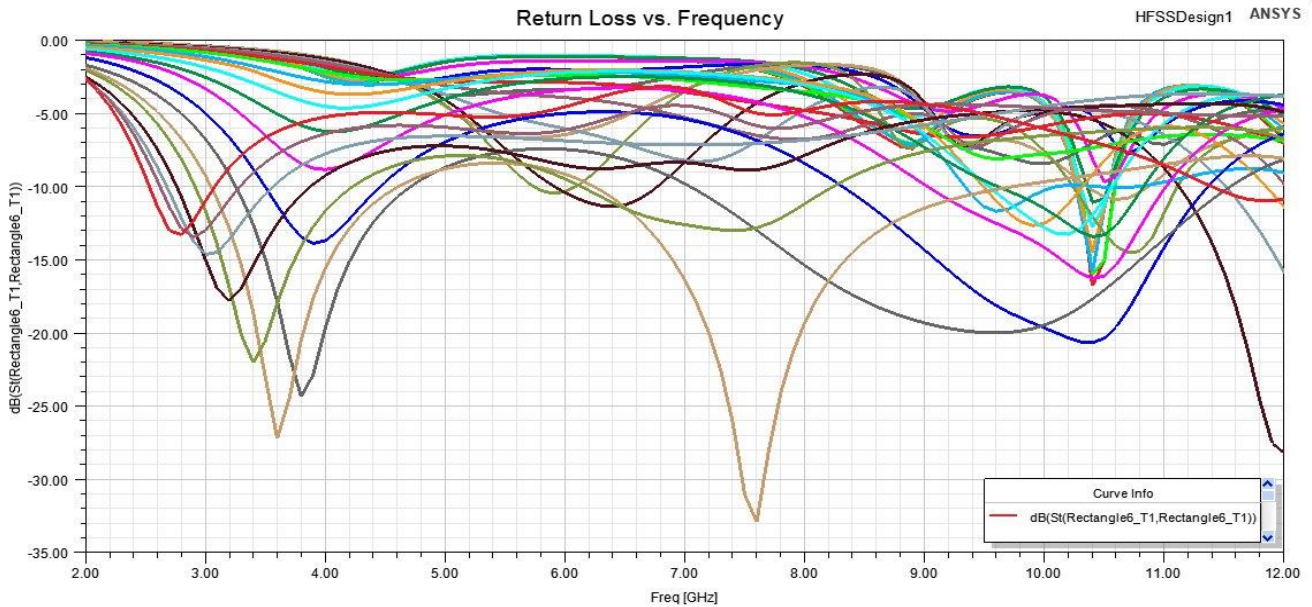


**Fig. 9 Parametric study for the partial ground plane**

**Table 3. Dimensions of the final radiating patch**

| Parameter | Value |
|---|---|
| Width of the patch ($W_p$) | 18mm |
| Length of the patch ($L_p$) | 20.25mm |
| Width of patch excluding first steps ($W_1$) | 9mm |
| Length of patch excluding first step ($L_1$) | 19.25mm |
| Width of patch excluding second steps ($W_2$) | 12mm |
| Length of patch excluding both steps ($L_2$) | 17.75mm |
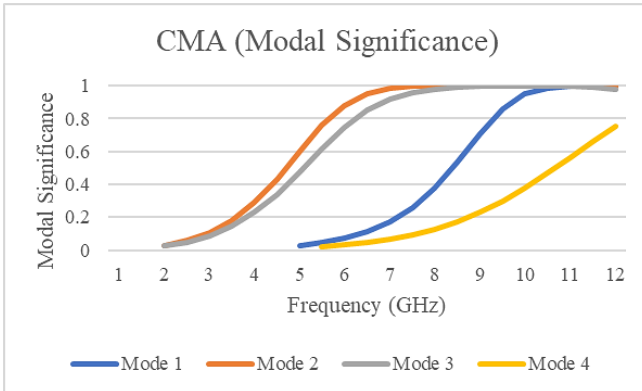


**Fig. 10 Modal significance vs. frequency plot for final patch geometry**

Additionally,

$$\beta_n = 180° - tan^{-1}(\lambda_n) \qquad (7)$$

where $\beta_n$ is the characteristic angle of $n^{th}$ mode. For a resonant mode, the eigenvalue is equal to 0, modal significance is equal to 1, and the characteristic angle is equal to $180°$.
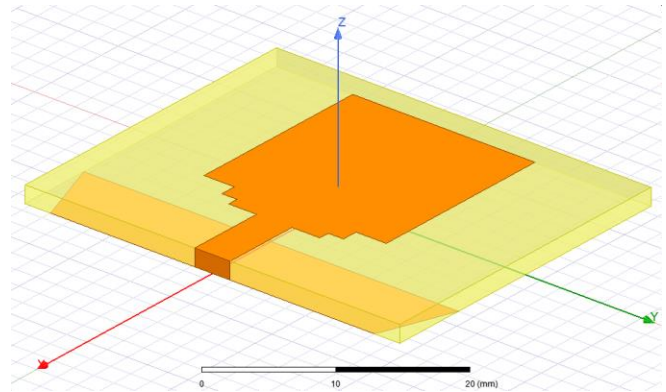


**Fig. 12 3D geometry of the proposed antenna**

For energy-storing inductive mode $\lambda_n > 0$, $90° < \alpha_n < 180°$. For energy-storing capacitive mode $\lambda_n < 0$, $180° < \alpha_n < 270°$. For both energy-storing modes, modal significance is away from the value 1 and near towards 0 or for extreme cases it is exactly equal to 0.

# 3. Antenna Design
## 3.1. CMA of Initial Radiating Patch

Initially, to find the characteristic modes of the radiating patch, the CMA is performed on a rectangular patch having a length of 14.46 mm and a width of 16.66 mm. These dimensions for 9GHz frequency are set up using the empirical equations given here.
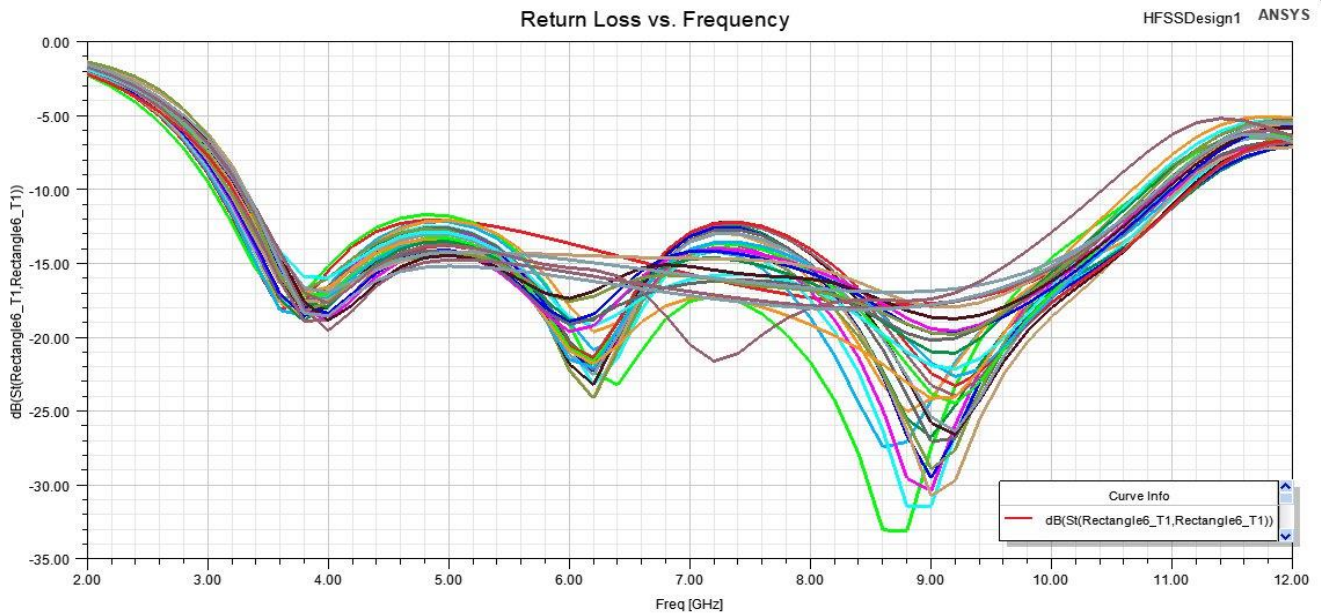


**Fig. 11 Parametric study for partial ground plane truncation**
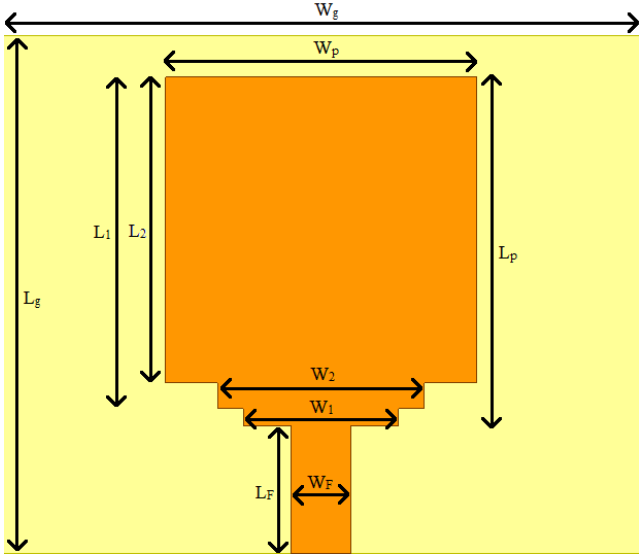
**Fig. 13 Top view of proposed antenna geometry**

$$Width(W) = \frac{c}{2f0\sqrt{\frac{\varepsilon R+1}{2}}} \qquad (8)$$

$$\varepsilon_{eff} = \frac{\varepsilon_R+1}{2} + \frac{\varepsilon_R-1}{2}\left[\frac{1}{\sqrt{1+12\left(\frac{h}{W}\right)}}\right] \qquad (9)$$
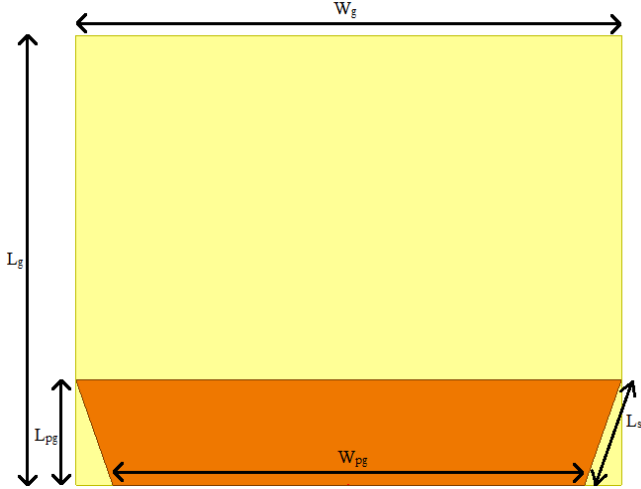


**Fig. 14 Bottom view of proposed antenna geometry**

$$Length(L) = \frac{c}{2f_0\sqrt{\varepsilon_{eff}}} - 0.824h\left[\frac{\left(\varepsilon_{eff}+0.3\right)\left(\frac{W}{h}+0.264\right)}{\left(\varepsilon_{eff}-0.258\right)\left(\frac{W}{h}+0.8\right)}\right] \quad (10)$$

In Equation 8, Equation 9, and Equation 10, $c$ is the speed of light, $f_0$ is resonance frequency, $\varepsilon_R$ is relative dielectric constant, $\varepsilon_{eff}$ is effective dielectric constant, $h$ is substrate height, $L$ is the length of the patch, and $W$ is the width of the patch. The purpose here is to find the natural characteristic modes, so the value of $\varepsilon_R$ is taken equal to 1, the value of $h$ is taken equal to 1.6mm (because that is going to be the substrate height of the final antenna), and as mentioned earlier the value of $f_0$ is taken equal to 9 GHz. The CMA

**Table 4. Design parameters for the proposed antenna**

| Parameter | Value |
|---|---|
| Width of the patch (W$_p$) | 18mm |
| Length of the patch (L$_p$) | 20.25mm |
| Width of patch excluding first steps (W$_1$) | 9mm |
| Length of patch excluding first step (L$_1$) | 19.25mm |
| Width of patch excluding second steps (W$_2$) | 12mm |
| Length of patch excluding both steps (L$_2$) | 17.75mm |
| Width of the partial ground plane (W$_g$) | 37mm |
| Width of the partial ground plane near feedline (W$_{pg}$) | 32mm |
| Length of the partial ground plane (L$_{pg}$) | 7mm |
| Slant Length of the partial ground plane (L$_s$) | 7.43mm |
| Substrate height (h) | 1.6mm |
| The relative dielectric constant of the substrate | 4.4 |
| Width of feed line (W$_F$) | 3.5mm |
| Length of feed line (L$_F$) | 7.375mm |

results for the radiating patch are shown in Figure 1 and Figure 2. It can be easily observed that Mode 1 and Mode 3 are resonant modes around 9 GHz because the eigenvalue is approximately 0 and the modal significance is approximately 1, which means that the structure can be easily excited at 9 GHz by exciting mode 1 and mode 3.

### 3.2. Steps/Stairs Creation and Optimization

For the wide impedance bandwidth, symmetric steps are created near the feed line.[23-24] Initially, the process starts with setting all the design parameters constant except any one (variable parameter). After that, the parametric analysis is performed on that variable parameter. The most appropriate and optimized value is selected for the variable parameter. This process is repeated until all the parameters are optimized. One additional thing to contemplate here is that the parametric analysis is not a simple bottom-up or top-down approach but also a cyclic and iterative one simultaneously.

The initial 3D design having the first step/stair is shown in Figure 3, and the top view of the same is shown in Figure 4. The parametric analysis for the first step/stair dimensions was performed, and the optimized value for the first step/stair turned out to be 1mm x 3mm. Table 1 contains different parameters and respective values for the structure shown in Figure 4. The dimensional values of the microstrip feed line are appropriately chosen for 50 Ohm impedance.

The second step is created in the patch to increase impedance bandwidth towards the UWB spectrum's high end. The top view of the design is shown in Figure 5. Figure 6 shows the parametric analysis for relation return loss vs. frequency, performed by taking constantly optimized dimensions for the first step and variable dimensions for the second step; the optimized value for the second step/stair turned out to be 1.5mm x 1.23mm. Table 2 contains only the dimensions related to the second step because the value of all other parameters is kept as same as in Table 1.

Performing CMA of this improved patch shows that it is possible to obtain wideband at the higher end of the UWB spectrum by appropriately exciting modes 1 and 2, as shown in Figure 7 and Figure 8.

### 3.3. Partial Ground Plane Creation and Optimization

The partial ground plane technique improves the return loss and impedance bandwidth at the lower end of the UWB spectrum. As the ground plane is larger than the patch, naturally, it resonates at a lower frequency. To find the optimum partial ground plane length, parametric analysis is performed, as shown in Figure 9. The optimum location of the partial ground plane is beneath the feed line with an optimized length ($L_{pg}$) of 7mm. Furthermore, some other sensible modifications to the patch dimensions are made to cover the entire frequency range, i.e., by creating multiple resonances over the spectrum. The final dimensions of the patch are shown in Table 3. The CMA for the final patch is also performed to understand modal excitation, and it can be easily observed in Figure 10 that by using appropriate feeding first three modes can be excited, each at different resonant frequencies of the UWB spectrum.

Lastly, to improve the reflection coefficient curve and bandwidth at the lower end of the UWB spectrum, right-angled triangle-shaped truncation of the partial ground plane is performed with the help of parametric analysis, as shown in Figure 11. The final 3D structure of the proposed antenna is shown in Figure 12, and the parameters with respective values are shown in Table 4. The top and bottom view of the proposed antenna is shown in Figure 13 and 14, respectively.

## 4. Results and Discussion

The proposed antenna is designed, simulated, and optimized using ANSYS Electronics Desktop 2020 R2. The performance of the proposed antenna is reported with the help of the reflection coefficient curve, voltage standing wave ratio (VSWR), and smith chart. A return loss of -10dB for wideband antennas is acceptable and corresponds to a VSWR of 2. It can be easily observed in Figure 15 that the proposed antenna covers the entire UWB spectrum. Also, both Figure 15 and Figure 16 show that the proposed antenna has an impedance bandwidth of 7.73GHz (3.04-10.77GHz). For the applications requiring better return loss (-15dB), the proposed antenna provides two bands, 3.38-4.02GHz (narrowband) and 5.67-9.95(wideband). In Figure 15, three main resonances can be
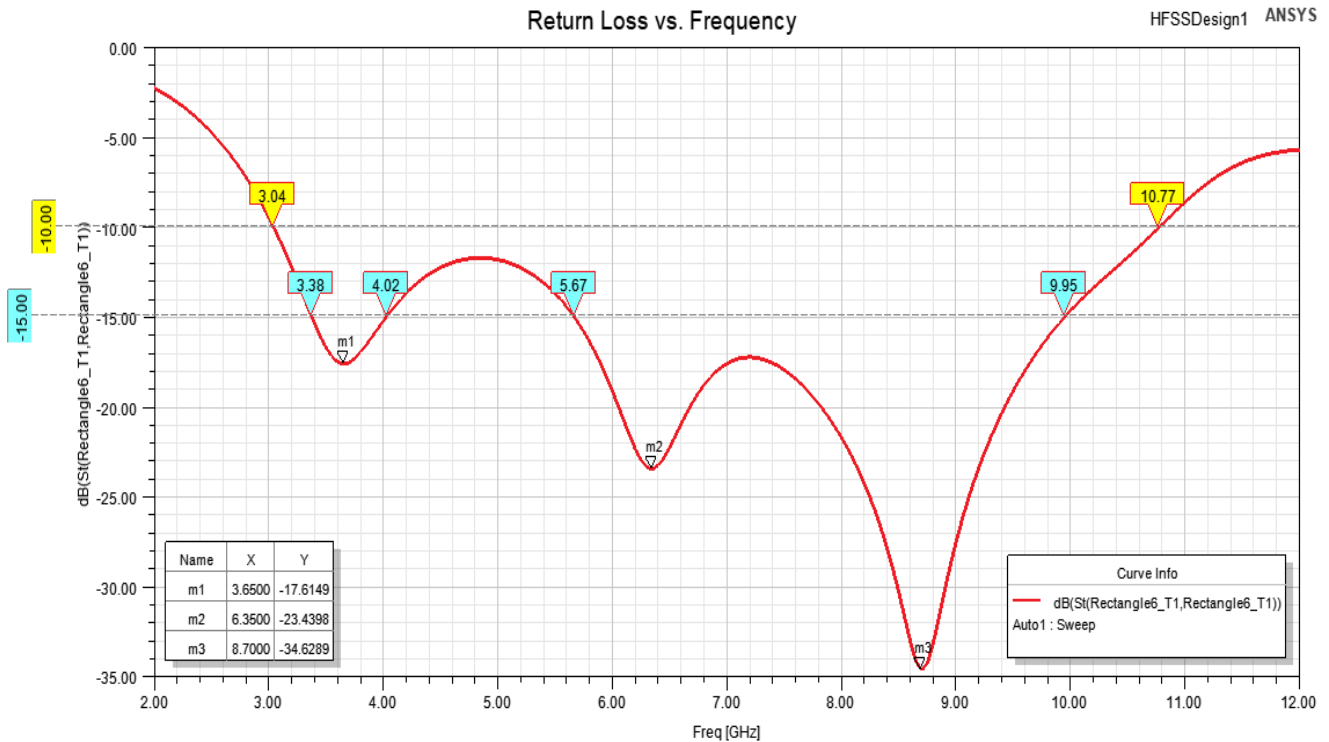


**Fig. 15 Reflection coefficient curve of the proposed antenna**
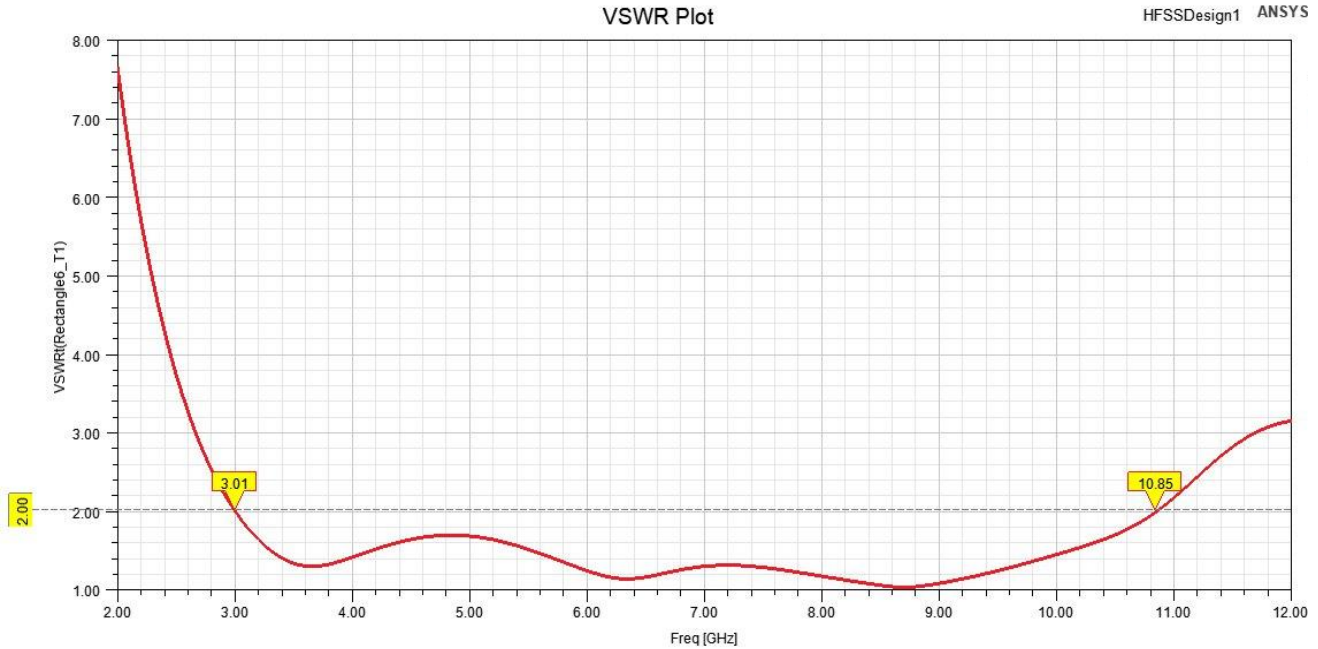
**Fig. 16 VSWR vs. frequency plot for the proposed antenna**

observed at 3.65GHz due to the truncated partial ground plane, at 6.35GHz and 8.7GHz due to the stepped patch. At 8.7GHz, return loss attains a value as good as approximately -35dB. The smith chart in Figure 17 shows that the matching is reasonably good over the entire UWB spectrum.

## 5. Comparative Study of Proposed Work with Existing Work

The comparative study of the proposed work with existing work is shown in Table 5. The working frequency range of the proposed antenna starts from 3.04GHz, where the return loss is -10dB. As the frequency increases from 3.04GHz, the return loss decreases, as shown in Figure 15. So, by offering a lower frequency at the lower end of the operating band than that of the UWB spectrum, the design provides better performance towards the edges of the UWB band.

## 6. Conclusion

**Table 5. Comparative Study**

| [Ref. No.] | Antenna Dimensions | Relative Dielectric constant | Antenna size | Operating Band |
|---|---|---|---|---|
| [25] | 40mm x 23.6mm | 4.4 | Moderate | 3-9.5GHz |
| [26] | 80mm x 80mm | 2.2 | Large | 2.35-6.1GHz |
| [27] | 30mm x 30mm | 4.4 | Small | 3.1-12GHz |
| [28] | 48mm x 40mm | 1.7 | Moderate | ≈ 3-12GHz |
| Proposed work | 30mm x 37mm | 4.4 | Small | 3.04-10.77 |
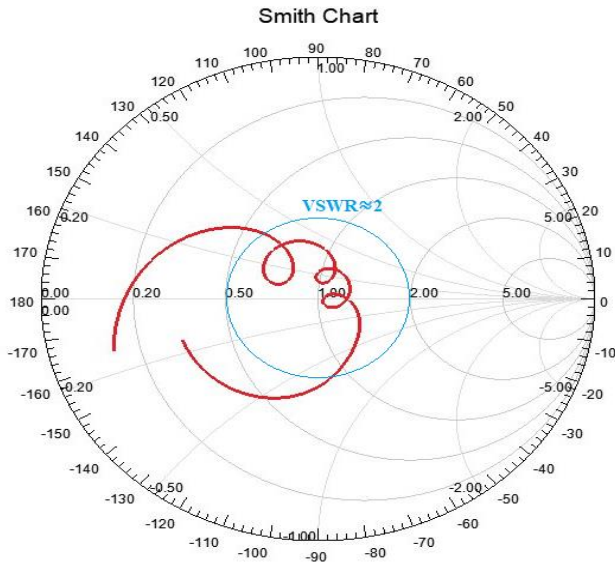
**Fig. 17 Smith chart for the proposed antenna**

The proposed UWB antenna design has an operating band of 3.04-10.77GHz, which is sufficient for any UWB communication application. For applications requiring better matching (lower return loss), the designed antenna also offers two specific bands, 3.38-4.02GHz and 5.67-9.95GHz. The applications of the proposed antenna design can be short-distance point-to-point communication, smart home applications, protected wireless payment systems, and other IoT applications.

## Conflicts of Interest

Our authors declare that there is no conflict of interest regarding the publication of this paper.

## References

[1] F. Nekoogar, "Ultra-Wideband Communications: Fundamentals and Application," 1st ed*., Hoboken: Pren. Hall*, vol.1, no.1, pp.1-17, 2005.

[2] B. Allen, M. Dohler, E. E. Okon, W. Q. Malik, A. K. Brown, and D. J. Edwards, "Ultra-Wideband Antennas and Propagation for Communications, Radar and Imaging," 1st ed., Chichester, England: *JW&S Ltd*, vol.1, no.1, pp.1-15, 2006.

[3] B. Silva, Z. Pang, J. Åkerberg, J. Neander and G. Hancke," Experimental study of UWB-based high precision localization for industrial applications," *in 2014 IEEE International Conference on Ultra-Wideband*, vol.1, no.12 , pp. 280-285.

[4] A. Ramos, A. Lazaro, D. Girbau, and R. Villarino, "RFID and Wireless Sensors Using Ultra-Wideband Technology," 1st ed., United Kingdom: Elsevier Ltd, vol.1, no.1, pp.1-18, 2016.

[5] 2015. arXiv website. [Online]. Available: https://arxiv.org/pdf/0911.1681.pdf

[6] H. Yoshioka, L. Yang, E. Tammam, and K. Yoshitomi, "A highly compact dual-band WLAN/UWB monopole antenna," *IEICE Elec.* Exp. Vol.9, no.3,  pp. 160-164, 2012.

[7] J. Deng, S. Hou, L. Zhao and L. Guo, "Wideband-to-Narrowband Tunable Monopole Antenna With Integrated Bandpass Filters for UWB/WLAN Applications," *IEEE Antennas and Wireless Propagation Lett.* Vol.16 , pp. 2734-2737, 2017.

[8] X. Shan and Z. Shen, "Miniaturized UHF/UWB Tag Antenna for Indoor Positioning Systems," *IEEE Antennas and Wireless Propag. Lett,* Vol.18, no.12, pp. 2453-2457, 2019.

[9] D. Manteuffel and R. Martens, "Compact Multimode Multielement Antenna for Indoor UWB Massive MIMO," *IEEE Transactions on Antennas and Propagation*, vol. 64, no.7, pp. 2689-2697, 2016.

[10] D. Potti, Y. Tusharika, M. G. N. Alsath, S. Kirubaveni, M. Kanagasabai, R. Sankararajan, S. Narendhiran, and P. B. Bhargav, "A Novel Optically Transparent UWB Antenna for Automotive MIMO Communications," *IEEE Transactions on Antennas and Propagation*, vol.69, no.7, pp. 3821-3828, 2021.

[11] R. Garbacz and R. Turpin, "A generalized expansion for radiated and scattered fields*," IEEE Trans. Antennas and Propag*, vol.19, no.3, pp. 348-358, 1971.

[12] C. Wang and Y. Chen, "Characteristic Modes: Theory and Applications in Antenna Engineering", 1st ed., *Hoboken: JW&S Ltd*, vol.1, no.1, pp.1-20.

[13] M. B. Perotoni, F. A. A. da Silva, and L. A. da Silva, "Characteristic Mode Analysis applied to antennas," *Rev. Bras. Ensino Fís*, vol.42, no.1, pp. 1-5, 2020.

[14] A. C. Suresh and T. S. Reddy, "Design of Corona Shaped 2x2 UWB-MIMO Antenna Using Characteristics Mode Analysis," International Journal of Engineering Trends and Technology, vol.70, no.2 , pp.260-269, 2022.

[15] R. Mittra, Ed., "Applications of the characteristic mode theory to antenna design, Developments in Antenna Analysis and Design," London, United Kingdom: *SciTech Publishing*, vol.1, no.1 , pp.1-31, 2018.

[16] R. Mittra, Ed., "Design of antennas mounted on complex platforms using the characteristic mode (CM) and characteristic basis (CB) function methods, Developments in Antenna Analysis and Design," London, United Kingdom: *SciTech Publishing*, vol.1, no.2, pp. 31-74, 2018.

[17] A. Mohanty and B. R. Behera, "Characteristics Mode Analysis: A review of Its Concepts, Recent Trends," *State-of-the-Art Developments and Its Interpretation with a Fractal UWB MIMO Antenna*, PIER B, vol. 92, no.1 , pp.19-45, 2021.

[18] W. Li, Y. Liu, J. Li, L. Ye, and Q. H. Liu, "Modal Proportion Analysis in Antenna Characteristic Mode Theory," *Int. J. Antennas Propag.* Vol.20, no.19, pp. 1-10, 2019.

[19] "Characteristic mode analysis: eigenvalue analysis of antenna structures," 2007. [Online]. Available: https://cerfacs.fr/wp-content/uploads/2016/03/rahola.pdf

[20] D. A. Strohschein, "Application of characteristic mode analysis to variable antenna placement on devices operating in the near -resonant range," Ph.D. thesis, *University of New Hampshire, Durha*m, NC, 2002.

[21] M. Cabedo-Fabres, E. Antonino-Daviu, A. Valero-Nogueira, and M. F. Bataller, "The theory of characteristic modes revisited: A contribution to the design of antennas for modern applications," *IEEE Antennas Propag*. Mag, vol.49, no.5, 52-68, 2007.

[22] D. Wen, Y. Hao, H. Wang, and H. Zhou, "Design of a Wideband Antenna with Stable Omnidirectional Radiation Pattern Using the Theory of Characteristic Modes," *IEEE Trans. Antennas Propag*, vol.65, no.5, pp. 2671-2676, 2017.

[23] S. K. Jain, S. Toshniwal, R. Purohit, "Design and Analysis of Rectangular Microstrip Antenna using Slotted Substrate Structure to Minimize Fabrication Error," *International Journal of Engineering Trends and Technology*, vol.15, no.9, pp.434-443, 2014.

[24] P. Kumar, N. Thakur, A. Sanghi, "Micro strip Patch Antenna for 2.4 GHZ Wireless Applications," *International Journal of Engineering Trends and Technology,* vol.4, no.8, pp.3544-3547, 2013.

[25] A. M. Ali, M. A. Al Ghamdi, M. M. Iqbal, S. Khalid, H. Aldabbas, and S. Saeed, "Next-generation UWB antennas gadgets for human health care using SAR," EURASIP *J. Wireless Com. Network*, vol.33, pp.1-20, 2021.

[26] C.-X. Zhang, Y.-Q. Zhuang, X.-K. Zhang, and L. Hu, "An UWB microstrip antenna array with novel corporate-fed structure," *Prog. In Electromagn. Res. C.,* vol.52, pp.7-12, 2014.

[27] A. A. Ibrahim and R. M. Shubair, "Reconfigurable band-notched UWB antenna for cognitive radio applications," *in 16th Mediterranean Microwave Symposium*, vol.41 , pp.14-16,2016.

[28] A. R. Hamza, A. Al-Hindawi, and H. I. Azeez, "Design and Analysis of Textile ISM/UWB Antenna for On-Body Communications," *J. Modelling Simulation Antennas Propag*, vol.2, no.1, pp. 7-12, 2016.